



HAL
open science

Bio-optical and biogeochemical properties of different trophic regimes in oceanic waters

Kadija Oubelkheir, Hervé Claustre, Antoine Sciandra

► **To cite this version:**

Kadija Oubelkheir, Hervé Claustre, Antoine Sciandra. Bio-optical and biogeochemical properties of different trophic regimes in oceanic waters. *Limnology and Oceanography*, 2005, 50 (6), pp.1795 - 1809. 10.4319/lo.2005.50.6.1795 . hal-01893852

HAL Id: hal-01893852

<https://hal.science/hal-01893852v1>

Submitted on 6 May 2021

HAL is a multi-disciplinary open access archive for the deposit and dissemination of scientific research documents, whether they are published or not. The documents may come from teaching and research institutions in France or abroad, or from public or private research centers.

L'archive ouverte pluridisciplinaire **HAL**, est destinée au dépôt et à la diffusion de documents scientifiques de niveau recherche, publiés ou non, émanant des établissements d'enseignement et de recherche français ou étrangers, des laboratoires publics ou privés.



Distributed under a Creative Commons Attribution 4.0 International License

Bio-optical and biogeochemical properties of different trophic regimes in oceanic waters

Kadija Oubelkheir, Hervé Claustre,¹ Antoine Sciandra, and Marcel Babin

Laboratoire d'Océanographie de Villefranche-sur-Mer, CNRS and Université Pierre et Marie Curie, 06238 Villefranche-sur-Mer, France

Abstract

To examine the source and magnitude of the variability of bio-optical properties in open ocean, we simultaneously measured inherent optical properties (IOPs) and biogeochemical quantities during late summer from the eutrophic waters of the Moroccan upwelling to the oligotrophic waters of the northwestern Mediterranean and the ultraoligotrophic waters of the eastern Mediterranean. Vertical distributions of spectral absorption and attenuation coefficients were measured with a high-resolution in situ spectrophotometer (WETLabs ac9) together with biogeochemical measurements that included phytoplanktonic pigments and particulate organic carbon concentrations, particle size distributions, and picoplankton abundance. The variability in specific IOPs (i.e., per unit of biogeochemical constituent concentration) was examined, and an optical index of particle size was derived. The fine-scale vertical distributions of various biogeochemical properties were thus described from ac9 profiles. Particle attenuation and carbon budgets, estimated from a combination of optical and biogeochemical measurements, underlie a major contribution of nonalgal stocks in oceanic waters. We show that first-order variations in IOPs in oceanic waters are explained by the trophic state (i.e., chlorophyll *a* concentration) and that second-order variations are the result of changes in the composition of phytoplankton assemblage, the balance between algal and nonalgal stocks, and light-related processes (colored dissolved organic material photo-oxidation and algal photo-adaptation).

At the interface between marine optics and biogeochemistry, bio-optical studies (Smith and Baker 1978) aim to characterize the biological and biogeochemical state of natural waters through their optical properties, and to quantify the role of the ocean in global biogeochemical (particularly carbon) budgets. These studies rely on the direct dependence of the water's inherent optical properties (IOPs) and apparent optical properties on the concentration and nature of optically significant biogeochemical constituents. In open ocean case I waters (Morel and Maritorena 2001 and references therein), these constituents are, by definition, phytoplankton and their accompanying and covarying retinue of material with biological origin, namely nonalgal particles (including biogenous detritus and heterotrophic organisms) and yellow substances (so-called colored dissolved organic material [CDOM]). Thus, optical properties generally are modeled as a function of chlorophyll *a* concentration (Chl *a*); used as a proxy for phytoplankton) in generic remote sensing algorithms for case I waters (Morel and Maritorena 2001 and

references therein). Such a simplified statement is, in a first approximation, verified on a global scale, but some nuances in the definition of case I waters must be introduced on a regional scale as the likely result of biogeochemical peculiarities at such levels (Morel and Maritorena 2001; Bricaud et al. 2002; D'Ortenzio et al. 2002). For a more accurate estimation of biogeochemical stocks from in situ or remote optical measurements, it is thus necessary to understand the source and magnitude of these regional specificities.

Total IOPs are the result of the additive contribution of light absorption and scattering by the individual optically significant constituents in the water. Absorption and scattering coefficients generally display specific spectral features or dependencies that might, in turn, be used to estimate the contribution of each constituent to the bulk measurement. Such deconvolution procedures rely on either experimental or numerical methods (Kishino et al. 1985; Gallegos and Neale 2002 and references therein; Schofield et al. 2004). After deconvolution, partial optical coefficients can be related to meaningful biogeochemical quantities if specific IOPs (i.e., IOPs per unit constituent concentration) are known. Thus, it is essential to fully understand and ultimately predict the regional and temporal variability of the relationships between optical properties and biogeochemical quantities.

Measurement of biogeochemical parameters, such as Chl *a* and organic carbon (particulate organic carbon [POC] and dissolved organic carbon [DOC] fractions) is essential for the description of spatiotemporal oceanic provinces and regional biogeochemical modeling for carbon-cycling studies. The variability in specific IOPs results from various sources. The variability in the Chl *a*-specific absorption coefficient of natural phytoplankton populations is statistically related to the trophic state (i.e., Chl *a* concentration) in oceanic waters, so Chl *a*-based parameterizations have been proposed

¹To whom correspondence should be addressed (claustre@obs-vlfr.fr).

Acknowledgments

We are grateful to Joséphine Ras and Jean Claude Marty for their contribution to pigment analysis and particulate absorption measurements and to Patrick Raimbault and Nicole Garcia for particulate organic carbon data. We also thank the crews of RV *Thalassa* for their support during field operations. We are grateful to Dominique Tailliez for CTD data acquisition and processing and to Bernard Gentili and Frank Fell for efficient discussions on computations. The ac9 data processing was conducted using the ADAM software (AC9 Data Manager; Informus GmbH). We also thank André Morel for fruitful discussions on an earlier draft. Comments by Emmanuel Boss and Grace Chang are acknowledged. K.O. benefited from a CNRS/Région PACA grant. This is a contribution of the PROSOPE group (PROOF-JGOFS-France).

to estimate this coefficient spectrally (Bricaud et al. 1995a, 1998). The DOC-specific dissolved absorption coefficient is highly variable in coastal and oceanic waters (Blough and Green 1995; Ferrari 2000; and references therein), mainly as a result of changes in the origin of dissolved material (terrestrial vs. oceanic) and CDOM photo-oxidation (into optically inactive forms of DOC) under high surface irradiances in stratified systems (Vodacek et al. 1997; Nelson et al. 1998). Recently, the effects of ultraviolet and visible radiation on the optical properties of CDOM were examined to model photo-oxidation kinetics in natural waters (Del Vecchio and Blough 2002). Finally, the variability in the POC-specific particle attenuation coefficient has been studied in various open ocean areas (Loisel and Morel 1998; Kinkade et al. 1999; Gardner et al. 2003 and references therein) using in situ single-wavelength transmissometers. Mishonov et al. (2003) recently underlined a small spatial and seasonal variability in this coefficient based on a data set covering a large range of trophic states.

Until recently, measurements of IOPs were performed using either laboratory spectrophotometers or in situ single-wavelength optical devices (e.g., transmissometers) in profiling mode to obtain spatial information with high resolution. The introduction of devices such as the spectral absorption-attenuation meter (WETLabs ac9 for nine wavelengths) has permitted the measurement of spectral absorption and attenuation coefficients in situ with a high spatial and temporal resolution (e.g., Bricaud et al. 1995b; Sosik et al. 2001; Twardowski and Donaghay 2001; Chang et al. 2002). Inverting IOPs measured by in situ spectrophotometers used in profiling mode into biogeochemical quantities is therefore a promising approach for addressing biogeochemical variability at observation scales that until now have been unattainable by conventional measurements (Barth and Bogucki 2000; Claustre et al. 2000). Determination of IOP profiles (using ac9s) together with discrete biogeochemical determinations have been conducted in coastal waters (Boss et al. 2001b; D'Sa and Miller 2003) and, more scarcely, open ocean waters (e.g., Claustre et al. 2000). The bio-optical variability of oceanic waters remains to be characterized over a large range of trophic states, which are representative of the expected variability in these waters.

The present study contributes to filling this gap. We analyzed an extensive data set of in situ spectral IOPs and biogeochemical measurements for a variety of open ocean waters, from the eutrophic waters of the Moroccan upwelling (UPW) to the ultraoligotrophic waters typical of the eastern Mediterranean. In situ continuous profiling of total and dissolved spectral absorption and attenuation coefficients was performed together with a suite of discrete optical and biogeochemical determinations, including phytoplankton pigments and POC concentrations, particle size distributions, and picoplankton numerical abundance. The resulting data set includes up to 1,000 samples for some discrete quantities and covers a large range of trophic states (greater than two orders of magnitude for many surface measurements), thus enabling us to address three essential topics: (1) the description of the variability in specific IOPs to understand how IOPs are shaped by biogeochemical stocks and, reciprocally, to what extent these stocks can be inferred from in situ pro-

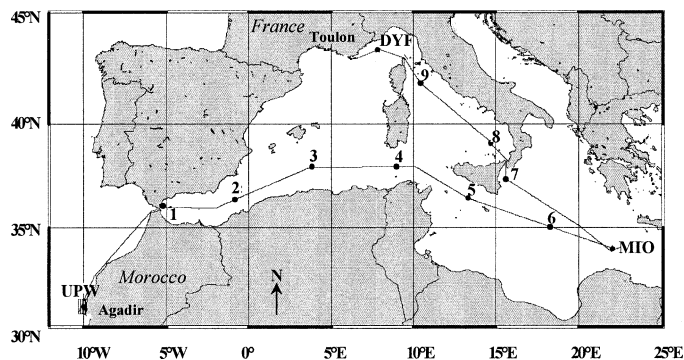


Fig. 1. Location of the stations visited during the PROSOPE cruise, from 4 September 1999 (Agadir, Morocco) to 4 October 1999 (Toulon, France). Two main types of stations were occupied: nine short stations (Sta. 1–9; occupied for 4 h around the solar noon) and three long stations (UPW, DYF, and MIO; occupied for more than 2 d). The line between stations represents the cruise track.

files of IOPs; (2) the comparative description at a fine vertical resolution of the bio-optical properties of three different trophic regimes in the context of prevailing environmental conditions; and (3) the building of a budget for the contribution by individual particle stocks (algal, heterotrophic, and detrital) to particle attenuation and, ultimately, POC stock, which is a key parameter in studies of the global carbon cycle. As a result of the diversity of trophic states covered by the present investigation (surface total Chl *a* concentration range, 0.03–3.75 mg Chl *a* m⁻³), it is expected that the acquired data set will allow us to draw general inferences relevant to open ocean waters.

Materials and methods

Sampled sites—Hydrographic, bio-optical, and biogeochemical data were simultaneously acquired from 4 September 1999 to 4 October 1999 aboard RV *Thalassa* during the PROSOPE cruise (French acronym for “PROductivité des Systèmes Océaniques PELagiques,” or “productivity of oceanic pelagic systems”). Two main types of stations were investigated (Fig. 1): (1) nine “short” stations (sampled for 4 h around the solar noon; Stations (Sta.) 1–9), and (2) three “long” stations (sampled for more than 2 d) in the UPW, the Ionian Sea (MIO), and the northwestern Mediterranean (DYF for Dyfamed site, the JGOFS French time-series site in the Mediterranean). The UPW will also be referred to as upwelling, and MIO and DYF will together be referred to as Mediterranean throughout the text.

Ac9 data acquisition—Two WETLabs ac9s were used to measure spectral attenuation and absorption coefficients at nine wavelengths (412, 440, 488, 510, 532, 555, 630, 676, and 715 nm). One was equipped with a 0.2- μ m Gelman Suporcap filter at the inlet of the measuring tubes to determine dissolved material optical coefficients ($a_g(\lambda)$ and $c_g(\lambda)$, notations in Table 1). The ac9s were attached to a Seabird carousel equipped with 21 Niskin sampling bottles (12 liters), a Seabird 911-Plus CTD, and a Chelsea fluorometer. This package was deployed between 0 and 400 m for Sta.

Table 1. Notations. The subscripts w, p, ϕ , nap, and g stand for pure water, particles, phytoplankton, nonalgal particles, and colored dissolved organic matter, respectively.

Parameter	Value
λ	Wavelength (nm)
$a(\lambda)$	Absorption coefficient measured by the ac9 (m^{-1}), equal to $a_t(\lambda) - a_w(\lambda)$ ($a_w(\lambda)$ is the pure water absorption coefficient)
$a_g(\lambda)$	Absorption coefficient of dissolved material measured by the ac9 (m^{-1})
$b(\lambda)$	Scattering coefficient measured by the ac9 (m^{-1}), equal to $b_t(\lambda) - b_w(\lambda)$ ($b_w(\lambda)$ is the pure water scattering coefficient)
$c(\lambda)$	Attenuation coefficient measured by the ac9 (m^{-1}), equal to $c_t(\lambda) - c_w(\lambda)$ ($c_w(\lambda)$ is the pure water attenuation coefficient)
$c_p(\lambda)$	Particle attenuation coefficient measured by the ac9 (m^{-1})
$\sigma_b(\lambda)$	Scattering cross-section ($\text{m}^2 \text{ cell}^{-1}$)
$\sigma_c(\lambda)$	Attenuation cross-section ($\text{m}^2 \text{ cell}^{-1}$)
$Q_c(\lambda)$	Efficiency factor for attenuation (dimensionless)
γ	Spectral particle attenuation exponent, estimated through $c_p(\lambda) = \alpha\lambda^{-\gamma}$
TChl <i>a</i>	Total chlorophyll <i>a</i> concentration, determined by HPLC, including mono- and divinyl-chlorophyll <i>a</i> as well as chlorophyll <i>a</i> isomer and epimer (mg m^{-3})
[Chl <i>a</i>]	Total chlorophyll <i>a</i> concentration, estimated through absorption coefficient at 676 nm (mg m^{-3}) as measured by the ac9
[POC]	Particulate organic carbon concentration (mg m^{-3})
$c_c^*(\lambda)$	Carbon-specific attenuation coefficient ($\text{m}^2 \text{ g C}^{-1}$)
C_s	Particle total geometric cross-section or surface concentration (m^{-1})
d_{mean}	Mean particle diameter (μm)
j	Junge exponent of the particle size distribution (computed in the 1.6–2.6 μm size range)
$c_\phi(\lambda)$	Phytoplankton attenuation coefficient (m^{-1})
$c_{\text{nap}}(\lambda)$	Nonalgal particle attenuation coefficient (m^{-1})
$c_{\text{het}}(\lambda)$	Heterotrophic attenuation coefficient (m^{-1})
$c_{\text{det}}(\lambda)$	Detrital attenuation coefficient (m^{-1})
$[C_\phi]$	Phytoplankton carbon concentration (mg m^{-3})
$[C_{\text{nap}}]$	Nonalgal carbon concentration (mg m^{-3})
$(C:\text{Chl } a)_\phi$	C:Chl <i>a</i> ratio for phytoplankton (g g^{-1})

1–9, DYF, and MIO and between 0 and 100 m for UPW. Profiles were conducted every 3 h over 5 days at DYF and MIO and over 36 h at UPW, with a vertical resolution of ~ 0.1 m (sampling rate, 6 Hz; profiling velocity, ~ 0.5 m s^{-1}).

Onboard the ship, both ac9s were calibrated twice during the cruise with optically pure water (MilliQ® A10 system) to quantify instrumental offsets. When corrected for these offsets, measured absorption ($a(\lambda)$) and attenuation ($c(\lambda)$) coefficients exclude the contribution by pure water (Table 1). Scattering by dissolved organic matter is assumed to be negligible so that dissolved absorption and attenuation coefficients are equivalent ($a_g(\lambda) \sim c_g(\lambda)$). This was confirmed by in situ measurements where $a_g - c_g < 0.006$ m^{-1} at all wavelengths. Time lags were applied to each profile to match up- and down-casts. Corrections for the in situ temperature

and salinity effects on the optical properties of water were applied as described by Pegau et al. (1997). Correction for incomplete recovery of the scattered light in the ac9 absorption tube was performed by subtracting $a(715)$ from $a(\lambda)$ (Zaneveld et al. 1994). Finally, ac9 data were averaged over 1-m intervals.

Data analysis revealed an instrumental drift over time (as already reported by Twardowski et al. 1999) monitored from the temporal evolution of $a(\lambda)$ and $c(\lambda)$ at 400 m in the Mediterranean (Oubelkheir et al. 2001; e.g., a drift of up to 0.06 m^{-1} was noticed for $c(440)$ over 2 weeks of intensive measurements). Absorption and attenuation spectra determined at this depth just after an absolute calibration (with optically pure water) were used as “references” (i.e., all spectra subsequently measured at 400 m were constrained to be always equal to these reference spectra). Any subsequent deviation of the measured coefficients at 400 m from these references was considered to result from the instrumental drift. This deviation was thus applied as a correction factor over the entire profile. This procedure is equivalent to that developed by Loisel and Morel (1998) for $c(660)$, except that they constrained the coefficient to be zero at a fixed depth. In the present study, the coefficients were constrained to more realistic values. The choice of 400-m waters as a reference was guided by the hydrological and optical stability (these waters correspond to Levantine Intermediate Waters; e.g., Millot 1999).

The particle attenuation coefficient ($c_p(\lambda)$) was computed as the difference between the measured attenuation and dissolved attenuation coefficients ($c(\lambda) - c_g(\lambda)$). The spectral dependency of $c_p(\lambda)$ was modeled according to an hyperbolic function (Van de Hulst 1957; Boss et al. 2001a and references therein) using a nonlinear regression method:

$$c_p(\lambda) = \alpha\lambda^{-\gamma} \quad (1)$$

where γ is the slope of the spectral dependency and α is a scaling factor.

Discrete data acquisition—Water samples were regularly collected for various discrete biogeochemical measurements. After filtration of seawater (1–5.6 liters, depending on samples) through Whatman GF/F glass-fiber filters, phytoplankton pigments were analyzed aboard ship by high-pressure liquid chromatography (HPLC) according to the method described by Claustre et al. (2004). The POC concentration was determined using a semiautomatic wet-oxidation method (Raimbault et al. 1999) after filtration of 1 liter of seawater onto precombusted Whatman GF/F glass-fiber filters. Autotrophic picoplankton, heterotrophic bacteria, and virus enumeration was performed on seawater samples fixed with 0.1% glutaraldehyde using a flow cytometer (FACSort; Becton Dickinson) according to the protocols described by Marie et al. (1999, 1997).

Particle size distributions were measured using an HIAC optical counter (Royco; Pacific Scientific). The measurement is based on the light-blockage principle. Further description of the counter principle and functioning has been given by Bernard et al. (1996). The various parameters used in the present study are defined here. If n_i is the number of particles counted in the size class i , then $N = \sum_{i=1}^m n_i$ is the total

number of particles counted in the sample volume V between the size classes $i = 1$ and $i = m$. The particle total geometric cross-section, equally named particle surface concentration (C_s), is thus defined as:

$$C_s = \frac{1}{V} \sum_{i=1}^m n_i s_g^i \quad (2)$$

where S_g^i is the geometric cross-section of the particles in the size class i . The particle mean diameter (d_{mean}) is:

$$d_{\text{mean}} = \frac{1}{N} \sum_{i=1}^m n_i \bar{d}_i \quad (3)$$

where \bar{d}_i is the diameter of the particles in the size class i . In the present study, the lower and upper size limits are 1.6 and 50 μm , respectively, and the counts are distributed within $m = 85$ log-normal size classes. The Junge exponent (j) is estimated from the slope of the linear regression on the log-transformed particle densities in the size range of 1.6 to 2.6 μm . The computation of j on this restricted range (11 size classes) was constrained by an instrumental artifact appearing around 2.6 μm (resulting from an uncertainty in the calibration curve of the HIAC particle counter around this domain). This Junge exponent is assumed to be representative of the size distribution of the particles that are most significant in scattering (Morel and Ahn 1991; Stramski and Kiefer 1991).

Finally, Q_b and Q_c (dimensionless) refer to the efficiency factors for scattering and attenuation, respectively, as defined as the ratios of the energy scattered or attenuated by a particle to the energy incident on its geometric cross-section s_g . The scattering and attenuation cross-sections (σ_b and σ_c) are, respectively, the products $s_g \times Q_b$ and $s_g \times Q_c$ (Van de Hulst 1957; Morel and Bricaud 1986).

Results and discussion

Inversion of optical properties into biogeochemical quantities—Absorption at 676 nm and Chl a concentration: Relationships between the total Chl a concentration, or [TChl a], and $a(676)$ generally are modeled using a power law function to account for the decrease of the chlorophyll-specific absorption coefficient with the increase in [TChl a], which is a consequence of the package effect and pigment composition change (Bricaud et al. 1995a). In the present study, the relationship between $a(676)_{\text{ac9}}$ and [TChl a] (Fig. 2A) is highly significant (Table 2) and can be expressed as:

$$[\text{TChl } a] = 67.8 a(676)_{\text{ac9}}^{1.16} \quad (4)$$

The UPW and Mediterranean data sets, analyzed separately, exhibited two relationships that are not statistically different, so $a(676)$ will be converted into [Chl a] using Eq. 4. The parameterization established on the PROSOPE data set differs significantly (Table 2) from the “global” parameterization established by Bricaud et al. (1995a) ([TChl a] = $105 a_{\phi}(676)^{1.19}$; nonlinear fit to a large data set collected in various oceanic areas and trophic states; [TChl a] range, 0.02–25 $\text{mg Chl } a \text{ m}^{-3}$). Differences could result from the fact that during the PROSOPE cruise, [TChl a] was measured exclusively by HPLC (but only for some cruises in

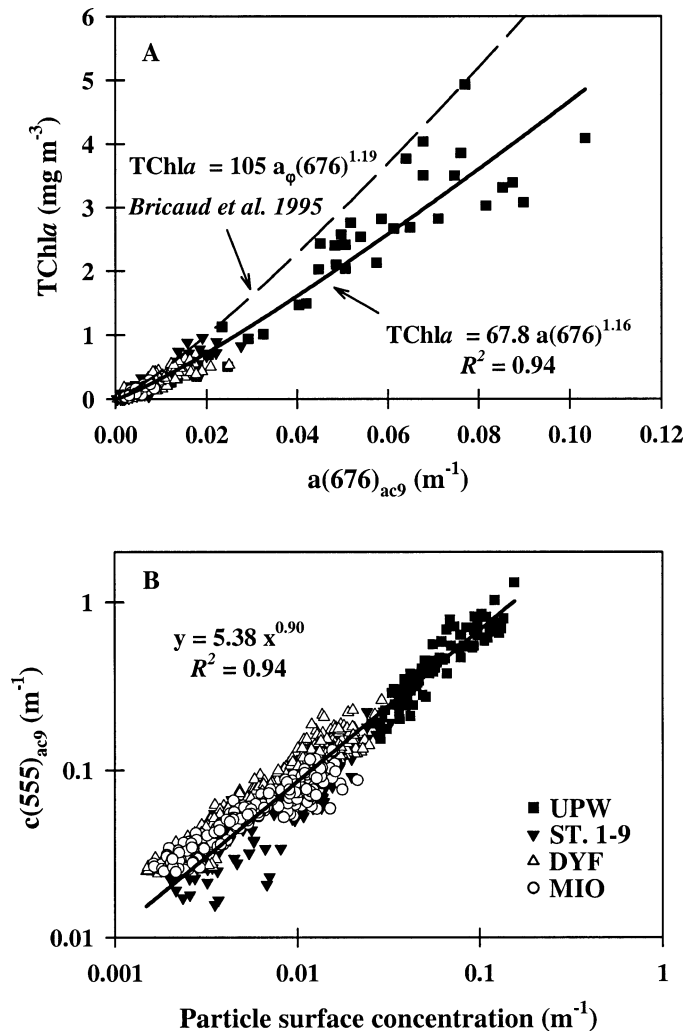


Fig. 2. Relationship between (A) the absorption coefficient measured by the ac9 at 676 nm ($a(676)_{\text{ac9}}$) and the HPLC-determined chlorophyll a concentration ([TChl a]) and (B) the attenuation coefficient at 555 nm measured by the ac9 ($c(555)_{\text{ac9}}$) and the particle surface concentration measured by the HIAC particle counter. Data from the entire PROSOPE data set (UPW, Sta. 1–9, DYF, and MIO) are shown.

Bricaud et al. 1995a), and $a(676)$ was measured using an ac9 (but the filter-pad technique in Bricaud et al. 1995a). Recently, Bricaud et al. (2004) extensively discussed the sources of variability in ($a_{\phi} - [\text{TChl } a]$) relationships based on a large data set of simultaneous HPLC pigments and filter-pad absorption determinations collected in various oceanic areas and trophic states (including the PROSOPE data set). They showed that regional deviations from global relationships are mainly caused by variations in the size structure of the algal community (i.e., package effect), whereas variations in the pigment composition are generally a second-order source of variability.

Particle attenuation (magnitude and spectral shape), concentration, and size: Because CDOM and algal absorptions were small compared with scattering in our data set at 555

Table 2. Statistical parameters of the relationships between IOPs and biogeochemical constituent concentrations. The type of model applied is given in parentheses. Nonlinear regression methods were used to avoid making assumptions about the behavior of the standard errors.

Relationship	No. of samples (depth)	r^2	Coefficients \pm standard error	p
$a(676)_{ac9}$ and [TChl a] ($y = bx^c$)	407 (0–200 m)	0.94	$b = 67.8 \pm 3.2$ $c = 1.16 \pm 0.02$	<0.0001 <0.0001
$c(555)_{ac9}$ and particle surface concentration ($y = bx^c$)	1083 (0–200 m)	0.94	5.4 ± 0.1 0.90 ± 0.01	<0.0001 <0.0001
$c(555)_{ac9}$ and [POC] Sta. 1–9, DYF, and MIO ($y = y_0 + ax$)	135	0.83	$y_0 = 0.0147 \pm 0.0031$ $a = 0.0020 \pm 0.0001$	<0.0001 <0.0001
$c(555)_{ac9}$ and [POC] UPW ($y = y_0 + ax$)	5 (0–60 m)	0.88	0.1567 ± 0.0328 0.0024 ± 0.0005	0.0175 0.0183

nm ($(a_g + a_\phi)(555) < 10\%$ of $c(555)$ at all stations), the attenuation coefficient was considered to be equivalent to the particle scattering coefficient ($c(555) \sim c_p(555) \sim b_p(555)$). Variations in the scattering coefficient are driven by the numerical concentration of the particles and, to a lesser extent, by their size distribution, index of refraction, and shape (e.g., Kitchen et al. 1982; Baker and Lavelle 1984). The comparison of the attenuation coefficient measured at 555 nm by the ac9 ($c(555)_{ac9}$) with the particle surface concentration (C_s , integrating both numerical concentration and size effects; see Eq. 2) reveals a significant covariation (Fig. 2B) that is described by a power law function (Table 2).

The particle attenuation efficiency factor ($Q_c(555)$) can be calculated from the ratio of $c(555)_{ac9}$ to the particle surface concentration (e.g., Morel and Bricaud 1986). Estimates of $Q_c(555)$ are higher in the Mediterranean ($Q_c \sim 14$) than in the upwelling ($Q_c \sim 3$) and, overall, are higher than the values predicted by the Van de Hulst anomalous diffraction approximation ($Q_c < 3$; Morel and Bricaud 1986). This overestimation, which increases with the proportion of smaller particles (from the upwelling to the Mediterranean), essentially occurs because the particle counter sees a finite size range (excluding pico-particles [diameter, $< 1.6 \mu\text{m}$]), whereas $c(555)$ integrates the contribution by all particles. Previous attempts to perform a closure between size distribution and particle attenuation/scattering measurements have generally failed (Claustre et al. 2000; Boss et al. 2001b) because of the difficulty in accounting for the “missing part” of the distribution or the part that is unseen by the particle counter (even assuming for pico-particles a Junge-type size distribution with an exponent equal to 4.5 and an index of refraction of 1.05; Claustre et al. 2000; present study, data not shown). This discrepancy points to the lack of knowledge regarding picoparticles, which represent a largely unknown stock that is potentially important in optical budgets (Stramski and Kiefer 1991; Claustre et al. 1999).

Further insights regarding the particle size can be obtained by analyzing the spectral dependency of the particle attenuation coefficient ($c_p(\lambda)$), which is characterized by γ (see Eq. 1). Mie theory predicts that under well-constrained conditions (i.e., nonabsorbing, spherical particles with a spec-

trally constant index of refraction), γ is linked to the Junge exponent of the particle size distribution (j) through $j = \gamma + 3$ (Van de Hulst 1957; Boss et al. 2001a and references therein). Such a theoretical relationship has been partially validated in situ for coastal waters (Boss et al. 2001b; Babin et al. 2003), but to our knowledge, no such analysis has been carried out for the open ocean. Recently, Boss et al. (2001a) showed that this relationship theoretically also applies for particles that are nonspherical, absorbing, or have an index of refraction that is spectrally variable for most conditions encountered in the ocean.

In the present study variations in γ are compared with variations in j for oligotrophic Mediterranean waters and with variations in the particle mean diameter (d_{mean} ; see Eq. 3) for upwelling waters (as in this last case, high phytoplankton abundance leads to a size distribution with one or more modes) (Fig. 3; note that j and γ are plotted in reversed scale). The value of γ is between 0.34 (surface UPW) and 2.8 (deep Mediterranean), and the value of j ranges between 3.5 and 5.5. These last values are consistent with those of previous studies (Boss et al. 2001a and references therein). In the Mediterranean, γ and j vertical distributions exhibit similar trends, and at MIO, the relationship between these quantities is close to theoretical expectations ($j = \gamma + 3$). In the upwelling, γ roughly covaries with d_{mean} along depth. The present study shows that estimations of the particle size in terms of d_{mean} or Junge exponent, depending on the trophic state of the waters investigated, are possible from routine measurements of γ profiles (using ac9s) in oceanic waters. The vertical variability in γ profiles will be discussed later.

Particle attenuation and POC concentration: Particle surface concentration is correlated with POC content (Verity et al. 1992). Therefore, the attenuation coefficient at 555 nm can also be used as a proxy for the POC concentration ([POC]). In the present study, $c(555)_{ac9}$ and laboratory-measured [POC] were significantly correlated for Mediterranean samples (Fig. 4; Table 2), leading to a conversion factor (c_c^*) equal to $2.02 \text{ m}^2 \text{ g C}^{-1}$ at 555 nm (equivalent to $1.76 \text{ m}^2 \text{ g C}^{-1}$ at 660 nm, derived by linear interpolation between values at 630 and 676 nm). These values are in agreement

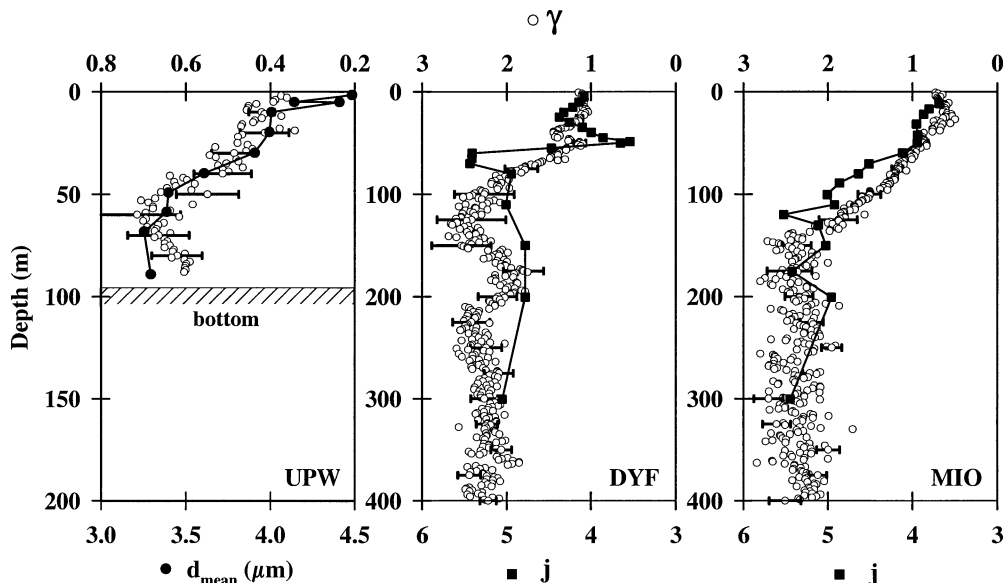


Fig. 3. Comparative vertical distributions of the spectral particle attenuation exponent measured by the ac9 (γ ; plotted in reversed scale), the particle mean diameter (d_{mean}) at UPW (cast 10), and the Junge exponent (j ; plotted in reversed scale) at DYF and MIO sites (casts 94 and 31, respectively) as measured by the HIAC particle counter. Standard deviations of the hyperbolic model ($c_p(\lambda) = \alpha\lambda^{-\gamma}$) adjustments are given each 10 m for UPW and each 25 m for DYF and MIO.

with $c_c^*(660)$ estimations in various oceanic areas based on direct POC determinations ($2\text{--}3.2 \text{ m}^2 \text{ g C}^{-1}$) (Loisel and Morel 1998; Mishonov et al. 2003; Fennel and Boss 2003; and references therein). By contrast, the UPW waters (Fig. 4; Table 2) are characterized by a slightly different c_c^* ($\sim 2.38 \text{ m}^2 \text{ g C}^{-1}$ at 555 nm and $\sim 2.33 \text{ m}^2 \text{ g C}^{-1}$ at 660 nm) and, in particular, a high intercept on the attenuation axis (0.157 m^{-1} at 555 nm and 0.125 m^{-1} at 660 nm). Such differences likely are caused by changes in the particle assemblage composition and associated changes in the size distribution and refractive index. As revealed by simultaneous pigments as

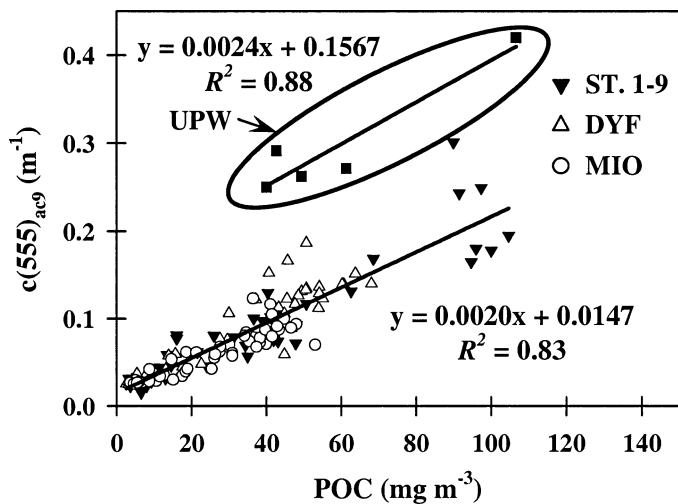


Fig. 4. Relationship between the attenuation coefficient at 555 nm measured by the ac9 ($c(555)_{\text{ac9}}$) and the laboratory-measured POC concentration for Mediterranean waters (Sta. 1-9, DYF, and MIO) and the Moroccan upwelling (UPW).

well as microscopic and cytometric determinations, micro-phytoplankton (mainly diatoms) dominates the algal fraction in the surface upwelling layer. In the Mediterranean, pico- and nano-phytoplankton are much more abundant. Values of c_c^* are known to vary as a function of phytoplanktonic groups and type of material (algal and nonalgal) and, thus, as a function of their respective proportion in natural particle assemblages (Claustre et al. 2002a). Diatoms present higher attenuation capabilities per unit of POC than nano- and pico-phytoplankton or nonalgal particles (*see below*). Diatoms are enclosed by a silica frustule and can form chains (as observed in the upwelling), which probably leads to a further increase of their attenuation capabilities. In the present study, POC will be derived from $c(555)$ using two different (local) relationships for the Mediterranean and the upwelling.

Bio-optical response to environmental conditions in oceanic waters—Environmental conditions: In what follows, the characteristics of the three long stations (UPW, DYF, and MIO) are analyzed in detail, because they encompass a range of trophic states that are representative of the potential diversity in oceanic waters. These three stations display different hydrological and chemical properties (Fig. 5). The upwelling is characterized by a weak stratification, with a nutrient-rich surface layer, whereas the Mediterranean presents a pronounced pycnocline (located at 20 m at DYF and 30 m at MIO) and nutrient-depleted surface waters (down to 30 and 80 m at DYF and MIO, respectively, for NO_3 ; Raimbault pers. comm.). The euphotic depth (i.e., the depth at which photosynthetically available radiation is reduced to 1% of its surface value) is, on average, 24, 51, and 82 m for UPW, DYF, and MIO, respectively (Hooker pers. comm.) (Fig. 5).

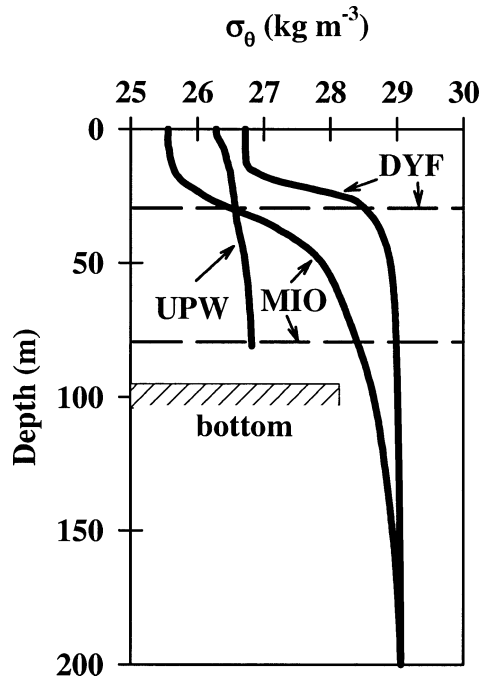


Fig. 5. Vertical mean density profiles (σ_θ) at UPW, DYF and MIO. The depth of the nitracline is also indicated for DYF and MIO (30 and 80 m, respectively).

Mean inherent optical properties spectra: The spectral variability in mean absorption and scattering coefficients was examined at the level of the chlorophyll maximum at UPW, DYF, and MIO (near the surface, at 45 and 90 m, respectively) (Fig. 6A,B; the spectra are normalized by their integral value). In the upwelling, the absorption spectrum (Fig. 6A) presents a marked algal contribution at 676 nm, whereas in the Mediterranean, the nonalgal contribution determines the general shape in spectral absorption (mainly CDOM, as evidenced by simultaneous CDOM and detrital absorption measurements; data not shown). Interestingly, the measured scattering spectra (Fig. 6B) are consistent with spectra simulated using Mie computations assuming an index of refraction of 1.05 and various Junge-type size distribution exponents (Babin et al. 2003) (Fig. 6C). At DYF and MIO, the Junge exponents used to simulate the measured spectra (~ 4.0 and ~ 4.2 , respectively) correspond to the Junge exponents estimated in situ (Fig. 3). At UPW, a Junge exponent lower than 3.4 must be assumed to reproduce the nearly flat spectra and the two minima at 440 and 676 nm (associated with the maxima in phytoplankton absorption; Van de Hulst 1957), which also compares to the Junge exponent estimated in situ (Fig. 3).

Bio-optical variability in different trophic regimes: As evidenced by optical measurements expressed in their biogeochemical equivalents, the UPW and the Mediterranean differ strongly in terms of particle and algal stocks (Fig. 7A,B), whereas CDOM (derived from $a_g(412)$) varies over a more restricted range (Fig. 7C). [Chl a] (derived from $a(676)$) varies over two orders of magnitude from MIO to UPW in the surface layer (0.03 – 3.9 mg Chl a m^{-3}) and one order of

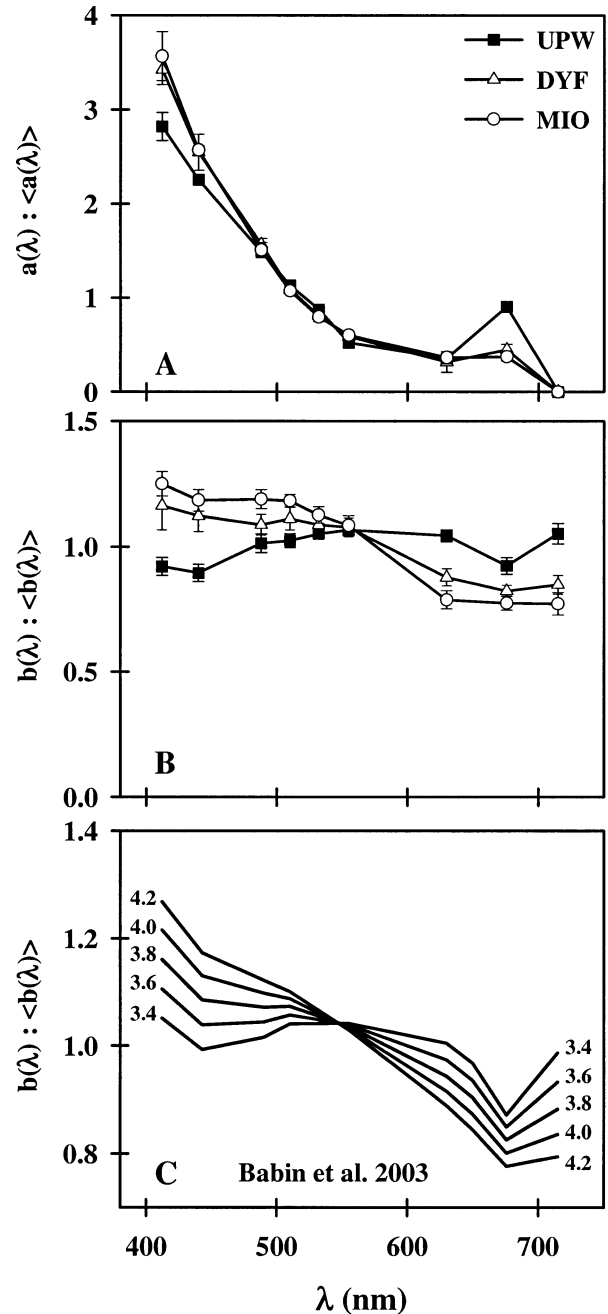


Fig. 6. Mean (A) absorption and (B) scattering spectra measured by the ac9 at the chlorophyll maximum at UPW, DYF and MIO ($n = 8, 35,$ and 31 casts, respectively; spectra are normalized by their integral; corresponding standard deviations are reported) are shown. Also shown are (C) scattering spectra simulated using Mie theory for algal particles, assuming various Junge-type size distribution exponents (j) ranging between 3.4 and 4.2 (Babin et al. 2003).

magnitude at the chlorophyll maximum (0.25 – 3.9 mg Chl a m^{-3}). Thus, these three sites are reasonably representative of most oceanic waters. By contrast, the [POC] (derived from $c_p(555)$) varies over less than one order of magnitude (28 – 175 mg C m^{-3} in the surface layer and 38 – 175 mg C m^{-3} at the maximum). The particle size (measured or optically

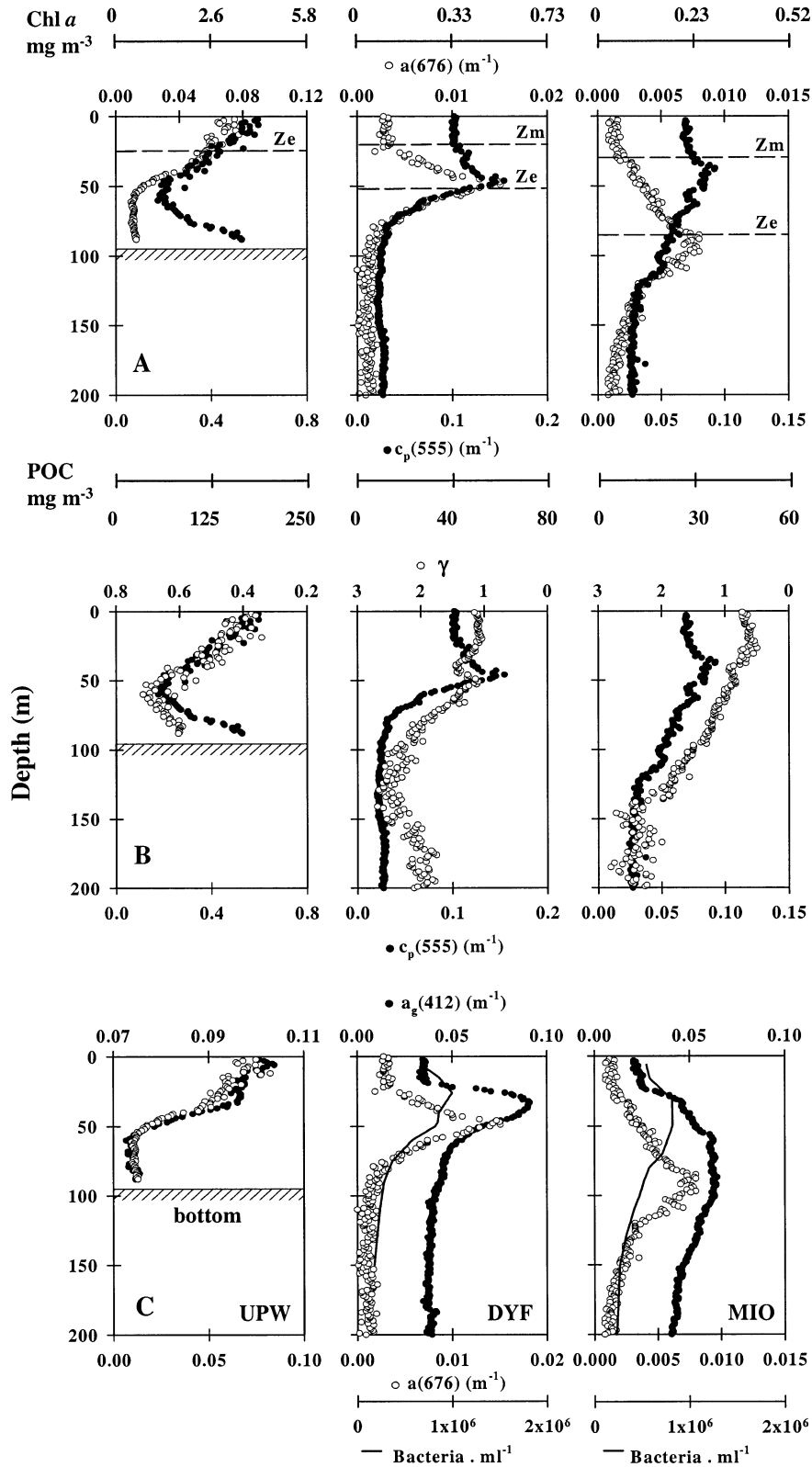


Fig. 7. (A) Comparative vertical distributions of the absorption coefficient at 676 nm ($a(676)$) and the particle attenuation coefficient at 555 nm ($c_p(555)$) at UPW, DYF, and MIO (casts 10, 94, and 31, respectively). Corresponding derived Chl a and POC concentrations are also shown. The depth of the euphotic zone (Z_e) and the lower limit of the mixed layer (Z_m) are indicated. (B) The spectral particle attenuation exponent (γ ; plotted in reversed scale) and the particle attenuation coefficient at 555 nm ($c_p(555)$). (C) The dissolved absorption coefficient at 412 nm ($a_g(412)$), the absorption coefficient at 676 nm ($a(676)$), and the heterotrophic bacteria abundance for DYF and MIO only.

derived from $c_p(\lambda)$ increases from the Mediterranean to the upwelling (Fig. 7B; at the POC maximum, $\gamma \sim 1.3, 0.8,$ and 0.34 at DYF, MIO, and UPW, respectively). The CDOM absorption at 412 nm (Fig. 7C) extends between 0.07 and 0.10 m^{-1} at UPW (in the bottom and surface layers, respectively) and 0.06 m^{-1} at MIO (depth, 60–90 m). The values measured in the upwelling fall within the range of values measured in other upwelling systems (Bricaud et al. 1981; Del Castillo and Coble 2000), whereas the maximum values measured in the Mediterranean are slightly higher than those encountered in similar trophic areas (Nelson et al. 1998 and references therein).

Superimposed on these general trends, the respective distributions of bio-optical properties are variable along the vertical scale (Fig. 7). In the upwelling, [Chl *a*], [POC], and CDOM covary within the surface layer (depth, 0–50 m) as a result of mixing. In this layer, the variability of bio-optical properties is driven by phytoplankton, the main source of CDOM (Bricaud et al. 1981) and particles. By contrast, in the bottom boundary layer (depth, >50 m), c_p significantly increases toward the bottom, whereas [Chl *a*] and CDOM remain constant. This increase in c_p with depth probably results from the presence of degraded algal material, as confirmed by an increase of the $a_\varphi(412) : a_\varphi(440)$ ratio (from 0.9 in the surface to 1.2 in the bottom; data not shown). Together with [POC], the particle size (optically derived) decreases from the surface to 50 m, suggesting that the surface layer is occupied by larger particles than are found in the bottom layer (as confirmed by discrete determinations). Although the upwelling is a mixed system, the mixing is not strong enough to homogenize the biogeochemical properties over the entire water column (0–90 m).

In the Mediterranean, [Chl *a*], [POC], and CDOM are clearly uncoupled along the vertical in the upper layer. Vertical distributions of POC and Chl *a* can be partitioned according to two layers at DYF (above and below the Chl *a* and POC maximum) and three layers at MIO (delimited by the deep chlorophyll and POC maxima). The vertical distribution of γ does not strictly follow the trends observed in POC (e.g., in the 0–50-m layer at DYF or the 0–40-m layer at MIO). Interestingly, the use of in situ spectrophotometers, such as the ac9, highlights some specific features that are not always captured using classical sampling strategies—for example, a layer of higher POC and particle size around 180 m at DYF. At both sites (DYF and MIO), CDOM subsurface maxima are located between the Chl *a* and heterotrophic bacteria maxima, and a surface deficit in CDOM is noticed. The observed vertical uncoupling between the various bio-optical properties (Chl *a*, POC, and CDOM) in the Mediterranean results from the balance between, first, processes related to light, such as algal photo-adaptation with depth (i.e., increase of intracellular pigment concentration and change in pigment composition with increasing depth; Fennel and Boss 2003 and references therein) and CDOM photo-oxidation in the surface layer (Vodacek et al. 1997; Nelson et al. 1998; Del Vecchio and Blough 2002) and, second, a probable distinct effect of nonalgal stocks and sources in shaping the vertical distribution of optical properties when the system becomes more oligotrophic. The vertical separation between the deep chlorophyll and algal biomass maxima caused by

algal photo-adaptation is a commonly observed feature in oligotrophic areas (Kitchen and Zaneveld 1990; Loisel and Morel 1998; Claustre et al. 1999; and references therein), and the mechanisms of its generation have been extensively discussed elsewhere (Fennel and Boss 2003 and references therein). By contrast, few authors have underlined the role of nonalgal stocks in shaping the optical properties in oligotrophic waters, such as bacteria in CDOM distributions (Nelson et al. 1998) and detritus and/or heterotrophs in particle attenuation distributions (Claustre et al. 1999 and references therein). Recently, Claustre et al. (2002b) also underlined the effect of large-scale, submicron Saharan (mineral) dust deposition in the variability of optical properties of the Mediterranean. These submicron particles probably are quantified, partly erroneously, as CDOM, which might explain the slightly higher CDOM absorptions observed in these waters (*see above*). For further insights regarding the effect of nonalgal stocks on bio-optical properties variability in oceanic waters, we attempted to estimate the respective contribution of individual particle stocks to particle attenuation in the various oceanic waters investigated.

Particle attenuation and POC budgets—The partial contributions of algal and nonalgal (detritus and heterotrophs) stocks to particle attenuation are assessed through estimations of the numerical abundance of the major phytoplanktonic and heterotrophic groups (using a flow cytometer and a particle counter) and through estimations of their scattering cross-sections, using a method proposed by Claustre et al. (1999). Scattering efficiency factors are computed through the anomalous diffraction approximation (Van de Hulst 1957) for “generic” cells, which are assumed to be representative of each population. The index of refraction is considered to be 1.05, and the mean diameters adopted in this study are reported on Table 3 together with the corresponding computed scattering cross-sections at 555 nm ($\sigma_b(555)$). For comparison, the mean diameters and $\sigma_b(555)$ values used in the study of Stramski et al. (2001) are also given. A sensitivity analysis of the particle attenuation budget to assumptions on the mean diameters assumed for these “generic” cells is presented later.

The algal fraction of c_p (c_φ) is computed as the sum of the partial contributions of each autotrophic group: $c_\varphi = c_{\text{pro}} + c_{\text{syn}} + c_{\text{pico}} + c_{\text{diato}}$, where the subscripts pro, syn, pico, and diato stand for *Prochlorococcus* sp., *Synechococcus* sp., picocoeukaryotes, and diatoms, respectively (m^{-1}). The contribution of microphytoplankton (mainly diatoms) to c_p (c_{diato}) is taken into account only in upwelling waters (negligible for the Mediterranean). The nonalgal fraction of c_p (c_{nap}) corresponds to the sum of heterotrophic and detrital stocks ($c_{\text{het}} + c_{\text{det}}$) and is computed as $c_{\text{nap}} = c_p - c_\varphi$. Then, under the assumption of a total heterotrophic contribution equal to twofold that of bacteria ($c_{\text{het}} = 2c_{\text{bact}}$; Morel and Ahn 1991; Claustre et al. 1999), the detrital fraction of c_p is estimated by difference ($c_{\text{det}} = c_p - c_\varphi - c_{\text{het}}$). To our knowledge, this is the first such estimation over a large range of trophic regimes and, in particular, in eutrophic waters (see Claustre et al. 1999 for a similar analysis of an oligotrophic regime).

The vertical distributions of computed partial attenuation

Table 3. Mean diameter adopted for *Prochlorococcus* sp., *Synechococcus* sp., picoeukaryotes, diatoms, and heterotrophic bacteria in the present study. Corresponding scattering cross-sections at 555 nm ($\sigma_b(555)$), computed through the anomalous diffraction approximation (Van de Hulst 1957; assuming an index of refraction equal to 1.05) are also reported. For comparison, the corresponding values used in Stramski et al. (2001) are reported in italic and parentheses.

Source		Mean diameter (μm)	$\sigma_b(555)$ ($\text{m}^2 \text{cell}^{-1}$)
<i>Prochlorococcus</i> sp.	Morel et al. (1993)	0.70 (0.66)	5.44×10^{-14} (4.02×10^{-14})
<i>Synechococcus</i> sp.	Morel et al. (1993)	1.20 (1.05)	4.55×10^{-13} (3.25×10^{-13})
Picoeukaryotes	Campbell and Vaulot (1993)	2.28	5.24×10^{-12}
Diatoms	Computed from HIAC particle size distributions	9.3 (7.73)	1.97×10^{-10} (9.12×10^{-11})
Heterotrophic bacteria	Morel and Ahn (1991)	0.5 (0.55)	1.43×10^{-14} (3.99×10^{-14})

values (c_φ , c_{het} and c_{det} ; m^{-1}) are displayed in Fig. 8, and their relative contributions to c_p are reported on Table 4. Various main observations are highlighted. At DYF, c_φ and c_p maxima are coincident and located at ~ 45 m, whereas at MIO, c_φ maximum is located in an intermediate position (depth, ~ 65 m) between the deep chlorophyll maximum and the particle maximum. The detrital contribution to c_p is dominant ($\sim 60\%$ at the particle maximum) whatever trophic system is considered, whereas the algal contribution to c_p increases from ultraoligotrophic to eutrophic waters (from 13% to 34% at the particle maximum), at the expense of the heterotrophic contribution. For the large trophic gradient investigated here, it would be a priori expected that the algal contribution to c_p increases at the expense of the nonalgal one (from oligotrophic to eutrophic). This is globally the case (Table 4), but some nuances have to be noted. First, the relative con-

tribution of detritus to c_p is stable whatever the trophic regime. This detrital material is, by contrast, weakly absorbing ($a_{\text{nap}}(440)/a_p(440) < 28\%$ at the chlorophyll maximum; data not shown). Second, the trend in the relative contribution of heterotrophs to c_p reflects changes in trophic state, whereas the corresponding absolute values remain rather stable (at the maximum, c_{het} remains $\sim 0.02 \text{ m}^{-1}$). Third, the increase in the relative contribution of phytoplankton to c_p from MIO to UPW is relatively small (less than a factor of two) (Table 4), despite an increase by one order of magnitude in the corresponding absolute values (c_φ) and in [Chl *a*] (at the chlorophyll maximum) (Figs. 7, 8).

The relative contributions of detritus to c_p computed here are similar to estimations made under oligotrophic conditions in the equatorial/tropical Pacific (Claustre et al. 1999 and references therein). In a simulation of ocean IOPs,

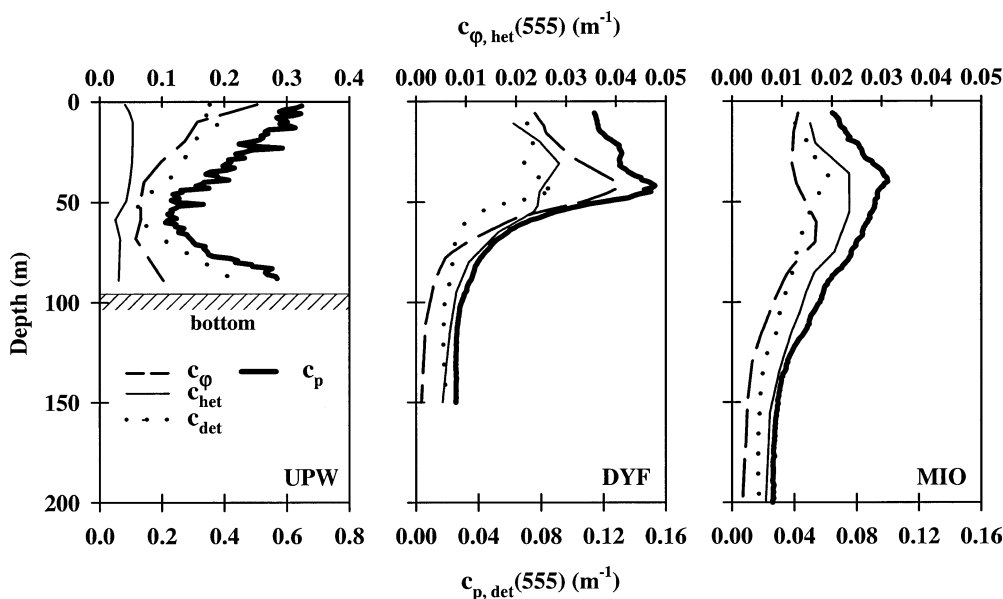


Fig. 8. Decomposition of particle attenuation coefficient into its major contributors (algal, heterotrophic, and detrital stocks) at UPW, DYF, and MIO (cast 10 at UPW; mean profiles at DYF and MIO, $n = 35$ and 31 casts, respectively).

Table 4. Relative contribution of phytoplankton, heterotrophs, and detritus to particle attenuation at 555 nm in the upwelling (UPW) at the level of the particle-chlorophyll maximum and in the bottom layer, and in the Mediterranean (DYF and MIO) at the level of the chlorophyll and particle maxima and in the 0–20-m layer. Note that the estimated contributions are sensitive to the mean diameters assumed for “generic” cells in the computations (*see text*). The range of variation in the algal (and, by difference, detrital) contribution is reported for varying phytoplankton mean cell diameters (6–13 μm for diatoms at UPW and 1–3 μm for picoeukaryotes at DYF and MIO; range reported in italic and parentheses).

Site	Layer	Phytoplankton (%)	Heterotrophs (%)	Detritus (%)
UPW	Chlorophyll-particle maximum (0–20 m)	34 <i>(diato: 6–13 μm)</i> 29–81	9	57 62–10
	Bottom layer (70–90 m)	19	7	74
DYF	Chlorophyll \sim particle maximum	27 <i>(pico: 1–3 μm)</i> 15–46	17	56 68–37
	0–20 m	22 <i>(pico: 1–3 μm)</i> 15–33	18	60 67–49
MIO	Deep chlorophyll maximum	17 <i>(pico: 1–3 μm)</i> 8–32	26	57 66–42
	Particle maximum	13 <i>(pico: 1–3 μm)</i> 6–25	23	64 71–52
	0–20 m	18 <i>(pico: 1–3 μm)</i> 10–31	22	60 68–47

Stramski et al. (2001), by varying the contributions of individual particles in a controlled manner, also evidenced a major contribution of nonalgal particles to scattering. By contrast, using the FCM-Mie method (a combination of Mie theory and flow cytometry), Green et al. (2003) estimated a major contribution of eukaryotic phytoplankton in surface waters of the continental shelf. The present study shows that picoparticles (*see above*), which correspond mainly to picodetritus (as shown in this section), play a major role in optical budgets and biogeochemical cycling in oceanic waters (present study; Green et al. 2003 and references therein), so their properties (e.g., size distribution and index of refraction) must be studied further. The picodetritus might correspond to broken cellular material (of phytoplankton origin) with a lower water content and, therefore, a higher index of refraction than would be found in living cells (Babin et al. 2003; Merien 2003).

A crucial assumption underlying the particle attenuation budget computed here and, thus, of all derived budgets (POC budget; *see below*) relies on the size assumed for each type of particle. Such assumptions were required, because the size distribution of individual micro-organisms was not estimated. Making such estimates is strongly recommended in future studies. We present here a sensitivity analysis of the c_p budget to variations in the mean cell size of picoeukaryotes (a main contributor to c_φ in oligotrophic areas; present study, data not shown; Claustre et al. 1999 and references therein) and heterotrophic bacteria in Mediterranean waters and of

diatoms in upwelling waters. Note that the detrital contribution to c_p is estimated as a “leftover” of the contributions from the major micro-organisms ($c_{\text{det}} = c_p - c_\varphi - c_{\text{het}}$) and, thus, is directly affected by under- or overestimations of algal or heterotrophic contributions (leading, respectively, to over- or underestimations of c_{det}).

In Mediterranean waters, we first varied the mean cell diameter of picoeukaryotes between 1 and 3 μm (this size range is representative of most oceanic picoeukaryotes populations; Simon et al. 1994). Results show that the corresponding detrital contribution to c_p varies at the particle maximum between 68% and 37% at DYF and between 71% and 52% at MIO (Table 4). Alternatively, we assumed a mean cell diameter of heterotrophic bacteria equal to 0.6 μm (whereas the mean diameter of picoeukaryotes was fixed at 2.28 μm). The c_{het} contribution ($2c_{\text{bact}}$) increases at the particle maximum to 35% at DYF and 48% at MIO. Note also that the assumption $c_{\text{het}} = 2c_{\text{bact}}$ (Morel and Ahn 1991) used in the present study was a main source of uncertainty and might not hold over the large range of water types explored here. For example, at MIO, there is a striking similarity between c_{het} and c_p vertical distributions (Fig. 8), which suggests that c_{het} is underestimated. Finally, in the upwelling, we varied the mean cell diameter of diatoms between 6 and 13 μm . Corresponding estimated algal contribution to c_p varies in the surface layer between 29% and 81%, respectively (Table 4). In conclusion, accurate determinations of the mean diameter and, ultimately, of the particle size dis-

Table 5. Carbon-specific particle attenuation coefficient for main phytoplanktonic groups encountered in open ocean waters and for nonalgal particles used in this study.

	Source	$c_c^*(660)$ ($\text{m}^2 \text{g}^{-1} \text{C}^{-1}$)
<i>Prochlorococcus</i> sp.	Claustre et al. (2002a)	1.0
<i>Synechococcus</i> sp.	Stramski et al. (1995)	2.5
Picoeukaryotes	DuRand and Olson (1998)	3.4
Diatoms	Stramski and Reynolds (1993)	3.8
Nonalgal particles	Claustre et al. (2002a)	1.5

tribution of the various types of particles acting in optical budgets are definitively required.

The c_p budget computed here can be converted into a carbon budget of the partial contributions of individual stocks to [POC] if the carbon-specific attenuation coefficients (c_c^*) for phytoplankton, heterotrophs, and detritus are known. Such estimation is of high interest to assess the role of individual particle stocks in organic carbon cycling in the ocean. Values for $c_c^*(660)$ used in the present study, derived from literature, are reported in Table 5. Because a similar spectral dependency is assumed for these various coefficients, $c_c^*(660)$ values are used directly to derive the POC budget. The [POC] attributed to each stock ($[C_{\text{stock}}]$) is estimated through c_{stock}/c_c^* . Algal carbon concentration ($[C_\varphi]$) is computed as the sum of the carbon concentration of each autotrophic group: $[C_\varphi] = [C_{\text{pro}}] + [C_{\text{syn}}] + [C_{\text{pico}}] + [C_{\text{diato}}]$. We found that nonalgal particles (heterotrophs and detritus) contribute approximately 80% of [POC], whatever the trophic system considered (Table 6). By contrast, phytoplankton represents only $\sim 20\%$ of [POC], which, again, is an unexpected result for the upwelling. At UPW, the decrease of algal contribution to POC relative to its contribution to c_p (c_φ contributes up to 34% of c_p in the surface layer) is a consequence of the predominance of diatoms in the phytoplankton assemblage (characterized by higher attenuation capabilities of the carbon biomass relative to other phytoplankton and nonalgal particles) (Table 5). The contribution of algal carbon to POC estimated here is similar to the values estimated in previous studies of other oceanic areas (DuRand et al. 2001 and references therein; Gundersen et al. 2001 and references therein). Note that the C:Chl a ratio for the sole algal material ($(\text{C}:\text{Chl } a)_\varphi$, g g^{-1}) can be derived from the ratio between algal carbon ($[C_\varphi]$, computed as detailed above) and optically derived Chl a (see Eq. 4) concentrations

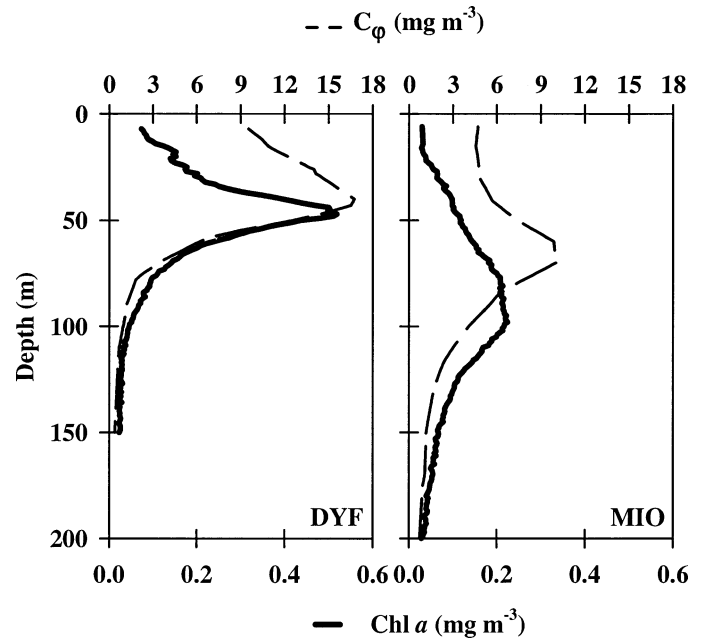


Fig. 9. Vertical distribution of the algal carbon ($[C_\varphi]$) and Chl a concentrations (derived, respectively, from the algal attenuation at 555 nm, $c_\varphi(555)$, and the absorption coefficient at 676 nm, $a(676)$) at DYF and MIO (mean profiles).

(Fig. 9) to examine the extent of algal photo-adaptation in Mediterranean waters. At the C_φ maximum, $(\text{C}:\text{Chl } a)_\varphi$ is between 42 g g^{-1} (at DYF) and 63 g g^{-1} (at MIO), which falls within the range of values reported for natural phytoplankton populations (Eppley et al. 1992 and references therein). Algal photo-adaptation is more marked at MIO than at DYF. At MIO, the algal carbon maximum is located at 65 m, or ~ 30 m shallower than the Chl a maximum and ~ 25 m deeper than the POC maximum. The algal C:Chl a is an essential variable (e.g., for biogeochemical modeling; Geider et al. 1998) and generally cannot be measured routinely, so the development of alternative methods, such as the one proposed in the present study, is highly relevant.

Interestingly, the “local” c_c^* value for the bulk material can be reconstructed if the c_c^* of individual particle stocks (Table 5) and their respective contribution to c_p (Table 4) are known and then compared to the measured c_c^* for the same bulk material. The computed c_c^* is 1.66, 1.83, and $2.42 \text{ m}^2 \text{g}^{-1} \text{C}^{-1}$ at the particle maximum at MIO, DYF, and UPW,

Table 6. Relative contribution of algal and nonalgal material to particulate organic carbon stocks in the upwelling (UPW) and in the Mediterranean (DYF and MIO).

Site	Layer	Phytoplankton (%)	Nonalgal material (heterotrophs + detritus) (%)
UPW	Chlorophyll-particle maximum (0–20 m)	22	78
DYF	Chlorophyll maximum \sim particle maximum	21	79
MIO	Deep chlorophyll maximum	19	81
	Particle maximum	14	86

respectively, which corresponds to ~82%, 91%, and 102% of the measured c_c^* in the Mediterranean and the upwelling (2.02, the global Mediterranean value, and 2.38 $\text{m}^2 \text{g C}^{-1}$ at 555 nm, respectively; *see above*). The agreement between the computed c_c^* (from c_c^* values of individual particle stocks and their respective contribution to c_p) and the measured c_c^* (derived from direct measurements on bulk material) represents an a posteriori validation of the assumptions made to derive the particle attenuation and carbon budgets. Note that these budgets were determined during late summer and, thus, represent a “snapshot” of the variability along time. Such estimations are required for various seasons in regions where the particle assemblage composition is highly variable over the year (e.g., temperate areas; Green et al. 2003).

The large range of trophic states explored here provides a unique opportunity to derive general trends in the bio-optical variability of open ocean waters. The present study confirms that Chl *a* explains the first-order variations in IOPs over the large range of conditions explored. Beside this expected result, the present study also emphasizes second-order sources of variability (i.e., nuances) in IOPs, namely the composition of phytoplankton assemblage, balance between algal and nonalgal stocks, and photochemical processes (e.g., CDOM photo-oxidation and algal photo-adaptation). These nuances might be better addressed and understood by the establishment of bio-optical databases, which would allow development of regional algorithms for the inversion of optical measurements (in situ or remote) into biogeochemical constituents (e.g., at the scale of the Mediterranean basin; Bricaud et al. 2002).

We believe that combining optical and biogeochemical information, as done in the present study, remains essential for a more accurate retrieval of biogeochemical parameters. These “combined” approaches allow development of regional algorithms that, in turn, are essential for the “all-optical” approaches that have been developed in the same areas. Exclusive use of optical instrumentation to address the variability in biogeochemical quantities, however, without any concurrent discrete measurement, is a highly attractive approach. The relative lack of accuracy in “all-optical” approaches can be considered to be compensated, at least in part, by the acquisition frequency, which allows addressing the biogeochemical variability at certain scales that have been unattainable using classical sampling strategies. For some remote platforms (e.g., mooring, drifters, autonomous underwater vehicles, and gliders; Dickey 2003), simultaneous validation by discrete measurements is, in most cases, not feasible; thus, the “all-optical” approaches will remain the only solution.

Besides such in situ studies, an important step in the accurate retrieval of biogeochemical properties from optical signals relies on the development of laboratory studies dedicated to specific particulate and dissolved pools. Phytoplankton has been the subject of intensive and exhaustive studies (Stramski et al. 2001 and references therein), but this has not been the case for many other stocks (e.g., heterotrophs and biodebris). Detritus and, more likely, biodebris probably represent a major and relatively stable contribution in optical (c_p) and biogeochemical (POC) budgets in oceanic waters. Deriving c_p and POC budgets from a combined ap-

proach using particle counts and individual particle properties (mean diameter, refractive index, and carbon-specific particle attenuation coefficient) is a powerful approach for optical and carbon-cycling studies. The recent development of automated submersible flow cytometers and their coupling with microscopy is thus promising for future carbon budgets at unprecedented temporal and spatial scales.

References

- BABIN, M., A. MOREL, V. FOURNIER-SICRE, F. FELL, AND D. STRAMSKI. 2003. Light scattering properties of marine particles in coastal and oceanic waters as related to the particle mass concentration. *Limnol. Oceanogr.* **48**: 843–859.
- BAKER, E. T., AND J. W. LAVELLE. 1984. The effect of particle size on the light attenuation coefficient of natural suspensions. *J. Geophys. Res.* **89**: 8197–8203.
- BARTH, J. A., AND D. J. BOGUCKI. 2000. Spectral light absorption and attenuation measurements from a towed undulating vehicle. *Deep-Sea Res.* **47**: 323–342.
- BERNARD, O., G. MALARA, AND A. SCIANDRA. 1996. The effects of a controlled fluctuating nutrient environment on continuous cultures of phytoplankton monitored by computers. *J. Exp. Mar. Biol. Ecol.* **197**: 263–278.
- BLOUGH, N. V., AND S. A. GREEN. 1995. Spectroscopic characterization and remote sensing of nonliving organic matter, p. 23–45. *In* R. G. Zepp and C. Sonntag [eds.], *The role of nonliving organic matter in the Earth’s carbon cycle*. Wiley.
- BOSS, E., M. S. TWARDOWSKI, AND S. HERRING. 2001a. Shape of the particulate beam attenuation spectrum and its inversion to obtain the shape of the particulate size distribution. *Appl. Opt.* **40**: 4885–4893.
- , AND OTHERS. 2001b. Spectral particulate attenuation and particle size distribution in the bottom boundary layer of a continental shelf. *J. Geophys. Res.* **106**: 9509–9516.
- BRICAUD, A., M. BABIN, A. MOREL, AND H. CLAUSTRE. 1995a. Variability in the chlorophyll-specific absorption coefficients of natural phytoplankton: Analysis and parameterization. *J. Geophys. Res.* **100**: 13321–13332.
- , E. BOSCH, AND D. ANTOINE. 2002. Algal biomass and sea surface temperature in the Mediterranean Basin. Intercomparison of data from various satellite sensors, and implications for primary production estimates. *Remote Sens. Environ.* **81**: 163–178.
- , H. CLAUSTRE, J. RAS, AND K. OUBELKHEIR. 2004. Natural variability of phytoplanktonic absorption in oceanic waters: Influence of the size structure of algal populations. *J. Geophys. Res.* **109**. [doi:10.1029/2004JC002419]
- , A. MOREL, M. BABIN, K. ALLALI, AND H. CLAUSTRE. 1998. Variations of light absorption by suspended particles with chlorophyll *a* concentration in oceanic (case 1) waters: Analysis and implications for bio-optical models. *J. Geophys. Res.* **103**: 31033–31044.
- , ———, AND L. PRIEUR. 1981. Absorption by dissolved organic matter of the sea (yellow substance) in the UV and visible domains. *Limnol. Oceanogr.* **26**: 43–53.
- , C. ROESLER, AND J. R. V. ZANEVELD. 1995b. In situ methods for measuring the inherent optical properties of ocean waters. *Limnol. Oceanogr.* **40**: 393–410.
- CAMPBELL, L., AND D. VAULOT. 1993. Photosynthetic picoplankton community structure in the subtropical north Pacific Ocean near Hawaii (station ALOHA). *Deep-Sea Res.* **40**: 2043–2060.
- CHANG, G. C., AND OTHERS. 2002. Nearshore physical processes and bio-optical properties in the New York Bight. *J. Geophys. Res.* **107**. [doi:10.1029/2001JC001018]

- CLAUSTRE, H., F. FELL, K. OUBELKHEIR, L. PRIEUR, A. SCIANDRA, B. GENTILI, AND M. BABIN. 2000. Continuous monitoring of surface optical properties across a geostrophic front: Biogeochemical inferences. *Limnol. Oceanogr.* **45**: 309–321.
- , AND OTHERS. 1999. Variability in particle attenuation and chlorophyll fluorescence in the tropical Pacific: Scales, patterns, and biogeochemical implications. *J. Geophys. Res.* **104**: 3401–3422.
- , AND OTHERS. 2002a. Diel variations in *Prochlorococcus* optical properties. *Limnol. Oceanogr.* **47**: 1637–1647.
- , AND OTHERS. 2002b. Is desert dust making oligotrophic waters greener? *Geophys. Res. Lett.* **29**. [doi:10.1029/2001GL014056]
- , AND OTHERS. 2004. An intercomparison of HPLC phytoplankton methods using in situ samples: Application to remote sensing and database activities. *Mar. Chem.* **85**: 41–61.
- D'ORTENZIO, F., S. MARULLO, M. RAGNI, M. R. D'ALCALA, AND R. SANTOLERI. 2002. Validation of empirical SeaWiFS algorithms for chlorophyll-*a* retrieval in the Mediterranean Sea. A case study for oligotrophic seas. *Remote Sens. Environ.* **82**: 79–94.
- D'SA, E. J., AND R. L. MILLER. 2003. Bio-optical properties in waters influenced by the Mississippi River during low flow conditions. *Remote Sens. Environ.* **84**: 538–549.
- DEL CASTILLO, C. E., AND P. G. COBLE. 2000. Seasonal variability of the colored dissolved organic matter during the 1994–95 NE and SW monsoons in the Arabian Sea. *Deep-Sea Res.* **47**: 1563–1579.
- DEL VECCHIO, R., AND N. V. BLOUGH. 2002. Photobleaching of chromophoric dissolved organic matter in natural waters: kinetics and modeling. *Mar. Chem.* **78**: 231–253.
- DICKEY, T. 2003. Emerging ocean observations for interdisciplinary data assimilation systems. *J. Mar. Syst.* **40–41**: 5–48.
- DURAND, M. D., AND R. J. OLSON. 1998. Diel patterns in optical properties of the chlorophyte *Nannochloris* sp.: Relating individual-cell to bulk measurements. *Limnol. Oceanogr.* **43**: 1107–1118.
- , ———, AND S. W. CHISHOLM. 2001. Phytoplankton population dynamics at the Bermuda Atlantic Time-Series station in the Sargasso Sea. *Deep-Sea Res.* **48**: 1983–2003.
- EPPLEY, R. W., F. P. CHAVEZ, AND R. T. BARBER. 1992. Standing stocks of particulate carbon and nitrogen in the equatorial Pacific at 150 degree W. *J. Geophys. Res.* **97**: 655–661.
- FENNEL, K., AND E. BOSS. 2003. Subsurface maxima of phytoplankton and chlorophyll: Steady-state solutions from a simple model. *Limnol. Oceanogr.* **48**: 1521–1534.
- FERRARI, G. M. 2000. The relationship between chromophoric dissolved organic matter and dissolved organic carbon in the European Atlantic coastal area and in the West Mediterranean Sea (Gulf of Lions). *Mar. Chem.* **70**: 339–357.
- GALLEGOS, C. L., AND P. J. NEALE. 2002. Partitioning spectral absorption in case 2 waters: Discrimination of dissolved and particulate components. *Appl. Opt.* **41**: 4220–4232.
- GARDNER, W. D., M. J. RICHARDSON, C. A. CARLSON, D. HANSELL, AND A. V. MISHONOV. 2003. Determining true particulate organic carbon: Bottles, pumps, and methodologies. *Deep-Sea Res.* **50**: 655–674.
- GEIDER, R. J., H. L. MACINTYRE, AND T. M. KANA. 1998. A dynamic regulatory model of phytoplankton acclimation to light, nutrients, and temperature. *Limnol. Oceanogr.* **43**: 679–694.
- GREEN, R., H. M. SOSIK, AND R. J. OLSON. 2003. Contribution of phytoplankton and other particles to inherent optical properties in New England continental shelf waters. *Limnol. Oceanogr.* **48**: 2377–2391.
- GUNDERSEN, K., K. M. ORCUTT, D. A. PURDIE, A. F. MICHAELS, AND A. H. KNAP. 2001. Particulate organic carbon mass distribution at the Bermuda Atlantic Time-Series Study (BATS) site. *Deep-Sea Res.* **48**: 1697–1718.
- KINKADE, C. S., J. MARRA, T. D. DICKEY, C. LANGDON, D. E. SIGURDSON, AND R. WELLER. 1999. Diel bio-optical variability observed from moored sensors in the Arabian Sea. *Deep-Sea Res.* **46**: 1813–1831.
- KISHINO, M., M. TAKAHASHI, N. OKAMI, AND S. ICHIMURA. 1985. Estimation of the spectral absorption coefficients of phytoplankton in the sea. *Bull. Mar. Sci.* **37**: 634–642.
- KITCHEN, J. C., AND J. R. V. ZANEVELD. 1990. On the noncorrelation of the vertical structure of light scattering and chlorophyll *a* in case I waters. *J. Geophys. Res.* **95**: 20237–20246.
- , ———, AND H. PAK. 1982. Effect of particle size distribution and chlorophyll content on beam attenuation spectra. *Appl. Opt.* **21**: 3913–3918.
- LOISEL, H., AND A. MOREL. 1998. Light scattering and chlorophyll concentration in case I waters: A reexamination. *Limnol. Oceanogr.* **43**: 847–858.
- MARIE, D., C. P. D. BRUSSAARD, R. THYRHAUG, G. BRATBAK, AND D. VAULOT. 1999. Enumeration of marine viruses in culture and natural samples by flow cytometry. *Appl. Environ. Microbiol.* **65**: 45–52.
- , F. PARTENSKY, S. JACQUET, AND D. VAULOT. 1997. Enumeration and cell-cycle analysis of natural populations of marine picoplankton by flow cytometry using the nucleic acid stain SYBR Green I. *Appl. Environ. Microbiol.* **63**: 186–193.
- MERIEU, D. 2003. Variabilité biooptique à différentes échelles spatiales et temporelles dans l'Atlantique nord-est: interprétations biogéochimiques. Ph.D. thesis, Université Pierre et Marie Curie.
- MILLOT, C. 1999. Circulation in the western Mediterranean Sea. *J. Mar. Syst.* **20**: 423–442.
- MISHONOV, A. V., W. D. GARDNER, AND M. J. RICHARDSON. 2003. Remote sensing and surface POC concentration in the South Atlantic. *Deep-Sea Res.* **50**: 2997–3015.
- MOREL, A., AND Y.-H. AHN. 1991. Optics of heterotrophic nanoflagellates and ciliates: A tentative assessment of their scattering role in oceanic waters compared to those of bacterial and algal cells. *J. Mar. Res.* **49**: 177–202.
- , ———, F. PARTENSKY, D. VAULOT, AND H. CLAUSTRE. 1993. *Prochlorococcus* and *Synechococcus*: A comparative study of their optical properties in relation to their size and pigmentation. *J. Mar. Res.* **51**: 617–649.
- , AND A. BRICAUD. 1986. Inherent optical properties of algal cells, including picoplankton. Theoretical and experimental results. *Can. J. Fish. Aquat. Sci.* **214**: 521–559.
- , AND S. MARITORENA. 2001. Bio-optical properties of oceanic waters: A reappraisal. *J. Geophys. Res.* **106**: 7163–7180.
- NELSON, N. B., D. A. SIEGEL, AND A. F. MICHAELS. 1998. Seasonal dynamics of colored dissolved material in the Sargasso Sea. *Deep-Sea Res.* **45**: 931–957.
- OUBELKHEIR, K. 2001. Caractérisation biogéochimique de provinces océaniques à l'aide d'indicateurs bio-optiques, à diverses échelles spatio-temporelles. Ph.D. thesis. Université de la Méditerranée.
- PEGAU, W. S., D. GRAY, AND J. R. V. ZANEVELD. 1997. Absorption and attenuation of visible and near-infrared light in water: Dependence on temperature and salinity. *Appl. Opt.* **36**: 6035–6046.
- RAIMBAULT, P., F. DIAZ, W. POUVESLE, AND B. BOUJELLAL. 1999. Simultaneous determination of particulate organic carbon, nitrogen, and phosphorus collected on filters, using a semiautomatic wet-oxidation method. *Mar. Ecol. Prog. Ser.* **180**: 289–295.
- SCHOFIELD, O., AND OTHERS. 2004. Inversion of spectral absorption

- in the optically complex coastal waters of the mid-Atlantic bight. *J. Geophys. Res.* **109**. [doi:10.1029/2003JC002071]
- SIMON, N., R. G. BARLOW, D. MARIE, F. PARTENSKY, AND D. VAULOT. 1994. Characterization of oceanic photosynthetic picoeukaryotes by flow cytometry. *J. Phycol.* **30**: 922–935.
- SMITH, R. C., AND K. S. BAKER. 1978. The bio-optical state of ocean waters and remote sensing. *Limnol. Oceanogr.* **23**: 247–259.
- SOSIK, H. M., R. E. GREEN, W. S. PEGAU, AND C. S. ROESLER. 2001. Temporal and vertical variability in optical properties of New England shelf waters during late summer and spring. *J. Geophys. Res.* **106**: 9455–9472.
- STRAMSKI, D., A. BRICAUD, AND A. MOREL. 2001. Modeling the inherent optical properties of the ocean based on the detailed composition of the planktonic community. *Appl. Opt.* **40**: 2929–2945.
- , AND D. A. KIEFER. 1991. Light scattering by microorganisms in the open ocean. *Prog. Oceanogr.* **28**: 343–383.
- , AND R. A. REYNOLDS. 1993. Diel variations in the optical properties of a marine diatom. *Limnol. Oceanogr.* **38**: 1347–1364.
- , A. SHALAPYONOK, AND R. A. REYNOLDS. 1995. Optical characterization of the oceanic unicellular cyanobacterium *Synechococcus* grown under a day-night cycle in natural irradiance. *J. Geophys. Res.* **100**: 13295–13307.
- TWARDOWSKI, M. S., AND P. L. DONAGHAY. 2001. Separating in situ and terrigenous sources of absorption by dissolved materials in coastal waters. *J. Geophys. Res.* **106**: 2545–2560.
- , J. M. SULLIVAN, P. L. DONAGHAY, AND J. R. V. ZANEVELD. 1999. Microscale quantification of the absorption by dissolved and particulate material in coastal waters with an ac-9. *J. Atmos. Ocean. Technol.* **16**: 691–707.
- VAN DE HULST, H. C. 1957. Light scattering by small particles. Wiley.
- VERITY, P. G., C. Y. ROBERTSON, C. R. TRONZO, M. G. ANDREWS, J. R. NELSON, AND M. E. SIERACKI. 1992. Relationships between cell volume and the carbon and nitrogen content of marine photosynthetic nanoplankton. *Limnol. Oceanogr.* **37**: 1434–1446.
- VODACEK, A., N. V. BLOUGH, M. D. DEGRANDPRE, E. T. PELTZER, AND R. K. NELSON. 1997. Seasonal variation of CDOM and DOC in the middle Atlantic bight: Terrestrial inputs and photo-oxidation. *Limnol. Oceanogr.* **42**: 674–686.
- ZANEVELD J. R. V., J. C. KITCHEN, AND C. MOORE. 1994. The scattering error correction of reflecting-tube absorption meters. *Proc. SPIE.* **2258**: 44–55.

Received: 29 March 2004

Accepted: 28 March 2005

Amended: 14 June 2005